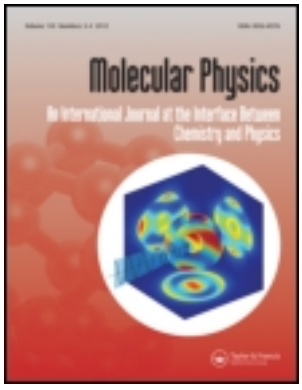

Molecular Physics: An International Journal at the Interface Between Chemistry and Physics
Publication details, including instructions for authors and subscription information:
http://www.tandfonline.com/loi/tmph20

Multi-fragment vector correlation imaging. A search for hidden dynamical symmetries in many-particle molecular fragmentation processes

F. Trinter [a], L.Ph.H. Schmidt [a], T. Jahnke [a], M.S. Schöffler [a d], O. Jagutzki [a], A. Czasch [a], J. Lower [a], T.A. Isaev [b], R. Berger [b], A.L. Landers [c], Th. Weber [d], R. Dörner [a] & H. Schmidt-Böcking [a]

[a] Institut für Kernphysik, Goethe-Universität Frankfurt, Max-von-Laue-Straße 1, D-60438 Frankfurt, Germany

[b] Clemens-Schöpf Institute for Organic Chemistry and Biochemistry, TU Darmstadt, Petersenstraße 22, D-64287 Darmstadt, Germany

[c] Department of Physics, Auburn University, Auburn, Alabama 36849, USA

[d] Lawrence Berkeley National Laboratory, Chemical Sciences, Berkeley, California 94720, USA

Accepted author version posted online: 26 Apr 2012. Version of record first published: 15 May 2012

To cite this article: F. Trinter, L.Ph.H. Schmidt, T. Jahnke, M.S. Schöffler, O. Jagutzki, A. Czasch, J. Lower, T.A. Isaev, R. Berger, A.L. Landers, Th. Weber, R. Dörner & H. Schmidt-Böcking (2012): Multi-fragment vector correlation imaging. A search for hidden dynamical symmetries in many-particle molecular fragmentation processes, Molecular Physics: An International Journal at the Interface Between Chemistry and Physics, 110:15-16, 1863-1872

To link to this article: http://dx.doi.org/10.1080/00268976.2012.686642

Molecular Physics
Vol. 110, Nos. 15–16, 10–20 August 2012, 1863–1872

INVITED ARTICLE

Multi-fragment vector correlation imaging. A search for hidden dynamical symmetries in many-particle molecular fragmentation processes

F. Trinter[a]*, L.Ph.H. Schmidt[a], T. Jahnke[a], M.S. Schöffler[ad], O. Jagutzki[a], A. Czasch[a], J. Lower[a], T.A. Isaev[b], R. Berger[b], A.L. Landers[c], Th. Weber[d], R. Dörner[a] and H. Schmidt-Böcking[a]

[a]*Institut für Kernphysik, Goethe-Universität Frankfurt, Max-von-Laue-Straße 1, D-60438 Frankfurt, Germany;* [b]*Clemens-Schöpf Institute for Organic Chemistry and Biochemistry, TU Darmstadt, Petersenstraße 22, D-64287 Darmstadt, Germany;* [c]*Department of Physics, Auburn University, Auburn, Alabama 36849, USA;* [d]*Lawrence Berkeley National Laboratory, Chemical Sciences, Berkeley, California 94720, USA*

(*Received 6 February 2012; final version received 12 April 2012*)

State-of-the-art multi-fragment imaging techniques like the COLTRIMS reaction microscope unveil the complete momentum pattern in low-energy atomic and molecular many-particle fragmentation processes much like the bubble chamber in high-energy particle physics. The excellent momentum resolution far below 1 $m_e a_0 E_h/\hbar$ (1 a.u.) and the high multi-fragment detection efficiency of the COLTRIMS technique reveal the dynamic correlation of bound many-particle systems as they are fragmented into the continuum. For the fragmentation process of carbon monoxide following carbon K-shell ionization using 306 eV photons (right and left circularly polarized) $h\nu + CO \rightarrow e_{photo} + O^+ + C^+ + e_{K\text{-}Auger,}$ the vector correlations between all fragments were measured in coincidence for each event. According to the common view of this process, the photoelectron and Auger electron emission probe different aspects of the time-dependent fragmentation process, i.e. the 'time evolution' of fragmentation. Based on measured vectors and vector combinations (e.g. vector products) of (1) the absorbed photon, (2) the emitted photoelectron and (3) ions, the Auger electron emission can be investigated with respect to the axes and planes defined by these vector combinations for each event in order to explore dynamical symmetries in multi-particle systems.

Keywords: vector correlation; four fragment momentum imaging; dynamical symmetries

1. Introduction

Many-particle quantum systems show features with astonishingly high correlation that are hard to predict and explain through simple dynamic properties of two-particle systems. In particular, when complex biomolecular processes are considered (e.g. the energy harvesting process of chlorophyll), one observes strict causal correlations between the initial and final states. In order to create such highly organized processes, unknown dynamic many-particle correlations may play a crucial role. Since the total linear and angular momentum of a closed quantum system are, according to current knowledge, always exactly conserved without any ambiguity caused by the uncertainty relation, the collective motion of many particles in a closed system (independent of the particle location) must ensure at *any instant* strict conservation of the total linear and angular momentum, i.e. the collective motion must be strictly connected. We speculate that there might even be a connection between the counterintuitive phenomenon of quantum entanglement in many-particle systems and unseen aspects of many-particle dynamics. Momenta are the only direct observables and can be measured for all fragments emitted in one process by the multi-coincidence technique with sub-atomic resolution without limitations. In contrast, the location of a particle for any given moment is not observable, hence it is from an empiricist perspective of science a metaphysical non-scientific concept.

Quantum theory currently describes many-particle dynamics with the modified dynamic laws established for two-particle systems. Despite the stunning success of this concept, one can never fully exclude the notion that correlated dynamics in four and more (many) particle systems might follow previously overlooked conservation laws. In theory, there is plenty of room to speculate, but experimental research has an advantage here. If there is a new experimental technique available, which has the power to search for such non-standard

*Corresponding author. Email: trinter@atom.uni-frankfurt.de

ISSN 0026–8976 print/ISSN 1362–3028 online

http://dx.doi.org/10.1080/00268976.2012.686642
http://www.tandfonline.com

behavior, it is clearly the obligation of an experimentalist to perform such experiments and, further, to search in many-particle systems for so far unknown additional dynamic conservation laws or symmetries. Therefore, measuring many-particle vector correlations may be a possible way to visualize such hidden dynamic properties [1,2].

In the pioneering work of Case and Herschbach [3] the investigation of vector correlations was used to explore, in a highly differential way, molecular collision dynamics. There, the initial state was prepared by means of laser techniques, thus up to four vector correlations could be measured. For example, in an atom plus diatom transfer reaction, the rotational angular momentum and the relative momenta of the reactants and products were measured. In the investigations of vector correlations performed thus far [3,4], typically only one scattered particle was detected in the final state and thus neither three nor four momentum vector correlations in the final state could be investigated. The approach presented here of vector correlation imaging can measure, by multi-fragment coincidence, four or more momentum vectors in the final state and thus allow investigations of symmetry in the complete final momentum space.

Atoms and molecules are the most suitable systems for such a search of unknown additional dynamic conservation laws or symmetries. In contrast to nuclear many-particle systems they are dominated by the well-understood Coulomb interaction. The fragmentation processes can be studied at energies far below any particle creation threshold and thus under extremely well-controlled conditions.

We demonstrate in this paper the multi-coincidence power of COLTRIMS (COLd Target Recoil Ion Momentum Spectroscopy) [5–9] for the carbon K-shell ionization of CO using left and right circularly polarized light followed by the emission of one Auger electron and fragmentation of the molecular dication,

$$h\nu(306\,\mathrm{eV}) + \mathrm{CO} \rightarrow \mathrm{e}_{\mathrm{photo}}(10\,\mathrm{eV}) + \mathrm{O}^+ + \mathrm{C}^+ + \mathrm{e}_{\mathrm{K\text{-}Auger}}(250\,\mathrm{eV}).$$

The momentum vectors of the four emitted fragments in the final state (two ions and two electrons) were determined, with the momentum of the Auger electron being calculated from the measured momentum vectors of the C^+ and O^+ ions as well as the photoelectron, using momentum conservation. Thus for each event, six vectors (initial state, incoming photon momentum and angular momentum vectors; final state, four momentum vectors) were determined.

At present, the data are not sufficiently accurate to make any conclusive statement on such symmetries, e.g. on time reversal or other symmetry laws in many-particle systems. However, we believe that the ideas should be reported here to stimulate further investigations on this topic and show preliminary data on such vector correlations in a four-particle molecular fragmentation process.

Modern experimental imaging techniques such as the COLTRIMS reaction microscope have reached such a powerful multi-fragment detection efficiency and excellent momentum resolution in fragmentation processes that speculative questions can indeed be explored experimentally [6–9]. Schmidt *et al*. [9] have recently shown that an overall recoil momentum resolution of 0.002 a.u. can be achieved in the 10 keV $H_2^+ + He \rightarrow H + H + He^+$ transfer ionization reaction. This is sufficient to detect tiny details of dynamic correlations.

In the above molecular fragmentation process the initial photon is absorbed by the molecule, accompanied by the instant emission of the low-energetic (10 eV) carbon K-photoelectron. During the fragmentation process the entire photon–molecule system remains entangled. This has recently been shown with a similar experiment on N_2, where gerade and ungerade intermediate states remain coherent throughout the fragmentation process [10]. In the present work we go further by considering a heteronuclear molecule like CO. The possibility of distinguishing the two atoms in this molecule establishes an additional directional vector. The incoming linear momentum of the photon (<0.1 a.u.) is transferred to the centre of mass of the system and not to the internal electronic molecular motion. However, the *angular* momentum of the photon is absorbed as internal angular momentum (the relative motion between the fragments). The entire fragmentation process is usually discussed using a multi-step picture [11]. (1) First, the photoelectron is emitted, leaving the molecule in a well-defined core hole state. (2) This state then decays a few femtoseconds later (several 100 atomic units) by emission of an Auger electron. (3) Finally, the doubly charged molecular ion Coulomb explodes. According to this simple model, the Auger electron should not carry any information on the direction of the photoelectron and, even more importantly, the Auger electron emission should be independent of the photon polarization. This latter point was questioned in Ref. [12], but more recent experiments in which the Auger electron was measured in the body fixed frame of the molecule showed no dependence of the Auger electron on the photon polarization [13] (see Figure 3 below). These previous tests of the simplified two-step model however were quite crude in the sense that the photoelectron was not observed. Recent experiments

on Ne K-shell ionization showed a surprising correlation between the photo and the Auger electron angular distributions that cannot yet be reconciled with standard post-collision interaction theory [14].

To explore the time sequence of such a fragmentation process (i.e. time symmetry), two possible experimental approaches are feasible. The first and more conventional is to refine the crude independent two-step picture to account for a possible causal interaction between the photoelectron and the Auger electron. Being the second emitted electron, the Auger electron might have a 'memory' of the fragmentation history. The Auger electron distribution therefore could depend on the photoelectron emission angle, i.e. on its direction of emission. The second approach is to analyse the momentum correlation between the Auger electron and the other measured vectors, i.e. the vector products of the photoelectron momentum $\boldsymbol{p}_{\text{ephoto,}}$ the momentum vectors of the ionic fragments $\boldsymbol{p}_{C+}$ or $\boldsymbol{p}_{O+}$ and the axial vector of the photon angular momentum $\boldsymbol{A}_{\text{photon}}$. This type of analysis is not motivated by any particular mechanistic scenario but by symmetry considerations only.

In our approach, all momenta of the charged fragments are measured in coincidence and are stored for each interaction in an event list (k, l, m, n) [15]. This method of data storage ensures that the photoelectron of event (k, l, m, n) is only correlated to fragments of the same event and never to any proceeding or subsequent events $(k, l, m, n \pm i)$. Therefore, one can calculate for each event the vector products and project the measured Auger distributions on axes or planes defined by these vector products. One example is the vector product $\boldsymbol{Z} = \boldsymbol{A}_{\text{photon}} \times \boldsymbol{p}_{\text{ephoto}}$. When mirroring the time from $t \rightarrow -t$ this new vector $\boldsymbol{Z}$ does not change its direction. That means that $\boldsymbol{Z}$ is even under time reversal (T-even). On the other hand, under spatial inversion, $\boldsymbol{r} \rightarrow -\boldsymbol{r}$, the vector $\boldsymbol{Z}$ is odd (P-odd). The Auger electron emission should show a perfect symmetrical distribution with respect to this $\boldsymbol{Z}$ direction if time is reversible in the Auger process. Measuring the Auger electron distributions for ($\boldsymbol{A}_{\text{photon}}(t)$ and $\boldsymbol{p}_{\text{ephoto}}(t)$) and for ($\boldsymbol{A}_{\text{photon}}(-t)$ and $\boldsymbol{p}_{\text{ephoto}}(-t)$), i.e. for left and right polarized photons and photoelectrons emitted in opposite directions, respectively, one can test the time inversion symmetry. The inversed Auger spectrum $(-t)$ should then be identical to that of (t). Table 1 presents other interesting combinations of vector products and scalar products with different behavior under P- and T-reversal (with $\boldsymbol{n}$ being the molecular vector pointing from the carbon nucleus to the oxygen nucleus).

Table 1. Vector products with respect to time and parity symmetries.

Vector product	$t \rightarrow -t$	$\boldsymbol{r} \rightarrow -\boldsymbol{r}$
$\boldsymbol{Z} = \boldsymbol{A}_\gamma \times \boldsymbol{p}_{\text{ephoto}}$	$\boldsymbol{Z}(t) = +\boldsymbol{Z}(-t)$	$\boldsymbol{Z}(\boldsymbol{r}) = -\boldsymbol{Z}(-\boldsymbol{r})$
$\boldsymbol{Z}' = (\boldsymbol{A}_\gamma \times \boldsymbol{p}_{\text{ephoto}}) \times \boldsymbol{p}_{\text{K-Auger}}$	$\boldsymbol{Z}'(t) = -\boldsymbol{Z}'(-t)$	$\boldsymbol{Z}'(\boldsymbol{r}) = +\boldsymbol{Z}'(-\boldsymbol{r})$
$S = (\boldsymbol{A}_\gamma \times \boldsymbol{p}_{\text{ephoto}}) \cdot \boldsymbol{n}$	$S(t) = +S(-t)$	$S(\boldsymbol{r}) = +S(-\boldsymbol{r})$

2. The COLTRIMS multi-fragment momentum imaging technique

Figure 1 shows an artist's view of the COLTRIMS reaction microscope. Fragmentation takes place in the intersection region of the photon beam and the supersonic gas jet. In a well-designed electric field configuration, the positively charged (red trajectories) and negatively charged (blue trajectory) fragments are projected (typically with 4π solid angle) towards two time- and position-sensitive detectors. Measuring the impact position for each fragment on the detector (typically <0.1 mm resolution) and its time-of-flight (typically <0.2 ns resolution) between the time of fragmentation and the impact on the detector, the particle trajectories and thus the particle momenta gained in the fragmentation can be determined. To improve the momentum resolution, electrostatic lenses (brown copper potential rings) can be incorporated into the spectrometer system. Trajectory calculations including such lenses can be found in Ref. [16]. Thus the influence of the extended target region, from where the fragments originate, can be strongly reduced [6–8].

Using particle detectors with fast delay-line position read-out, multi-fragment detection is possible [15]. Even two or more particles impacting on the same detector at the 'same' instant ($\Delta t < 1$ ns) can be detected simultaneously – as long as they are separated in space by at least 10 mm. The best multi-fragment detection can be obtained using modern transient recording techniques [15]. The data are acquired and stored in list mode event by event. Thus, for low-energy charged fragments (milli-eV to some eV) the COLTRIMS method is indeed a 4π imaging system. The rate of fragmentation processes that can be processed per second can approach 100 kHz.

To obtain 4π solid angle detection for particles with high transverse momentum, one has to ensure that the particles do not escape from the spectrometer. One way to achieve this is to increase the electric field. However, to obtain good momentum resolution, a long time-of-flight (i.e. a low electric field) is required. Thus for high-energetic electrons (above 100 eV) a magnetic field (parallel to the spectrometer axis) must be applied

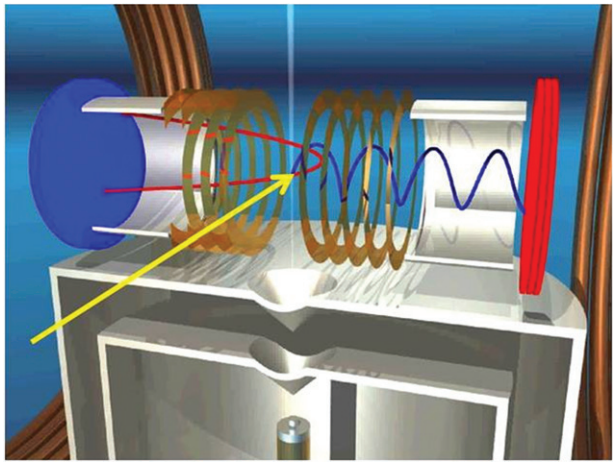

Figure 1. Artist's view of the COLTRIMS imaging system [6–8]. The axis of the spectrometer coincides with the z direction (time-of-flight of fragments), the supersonic jet with the y direction and the photon beam (yellow arrow) with the x axis.

in order to bend the electrons onto spiraling trajectories towards the detector [17]. Because the position x and y components are decoupled from the time-of-flight z component the initial momentum of the electron can still be deduced from the electron time-of-flight and position on the detector. Details of this technique are given in Refs. [5–9,15–17].

To ensure good momentum resolution for the ionic fragments, the target must have a well-defined momentum or be at rest in the laboratory frame. Thus cooling the target via a supersonic jet expansion or even laser cooling in a trap is crucial. As the cooling of heavy atoms and molecules to sub-Kelvin temperatures is sometimes difficult [18,19], a cold helium jet can be used as carrier medium. If all fragments of a molecular breakup are detected, it is possible to calculate the initial momentum of the molecule before the fragmentation, which allows for the reduction of the momentum uncertainty caused by the internal temperature of the target.

The high ionic momenta from the Coulomb explosion associated with the present experiment limited the ion detection to transverse momenta (in the x and y direction) smaller than ± 10 a.u. [5]. Because a Constant Fraction Discriminator [5,15] with a comparably slow timing digitizer (leading to a 20 ns dead time) was used instead of modern transient recording techniques, the double hit electron detection efficiency for two electrons emitted in the $+z$ direction was limited. In the case where both an Auger electron and a photoelectron are emitted in the z direction towards the electron detector, the high-energy Auger electron always arrives first and thus blocks the detection of the photoelectron with about 40% probability. This reduction of the Auger electron detection efficiency is fully symmetric around the $+z$ axis and should not influence the symmetry aspects with respect to the y and x direction. If, however, modern transient recorders are used (digitizing each time signal and storing the information) this blocking region would be strongly reduced to about 5 ns or a 5 mm blocking radius around the impact on the detector, which translates into a few percent loss of multiple electron hits only.

Since the data are stored in 'list mode' as discussed above, they can be transformed into any newly defined coordinate system, e.g. projected onto laboratory coordinates or projected onto axes or planes defined by the measured vectors or vector products. The coordinate systems used here are as follows.

Lab system: x is the direction of the incoming photon, so that its angular momentum vector points in the same (or opposite) direction. y is the direction of the gas jet and z is the direction of the COLTRIMS spectrometer axes, i.e. the direction of the time-of-flight measurement. Different vector correlation systems can be chosen: e.g. $x' = x$, y' and z' can be determined by the photoelectron momentum vector. This vector is always in the x'–y' plane and its z' coordinate is always zero.

Since for the measurement presented here a magnetic field was superimposed and a long ion spectrometer was used, the ion and electron trajectories (spirals) had larger uncertainties than anticipated. This limits the accuracy of the four particle vector correlations. Therefore, as mentioned above, no conclusions concerning possible symmetry violations can be made here and only the perspectives for future measurements are presented.

3. Data and discussion

The fragmentation of CO induced by circularly polarized photons has already been investigated by Jahnke *et al.* [20,21] and Weber *et al.* [13,22] for the same fragmentation process at the same photon energy. Thus we compare the present data with the previous results of Jahnke *et al.* and Weber *et al.* Jahnke *et al.* investigated the photoelectron distributions with respect to the molecular orientation. The molecular axis can be determined from the fragmentation axis of the Coulomb exploding molecule, if the fragmentation is much faster than the rotation of the molecular ion (i.e. the axial recoil approximation is valid [23]). Weber *et al.* have shown for the $C^+ + O^+$ channel that the region of high kinetic energy release (KER)

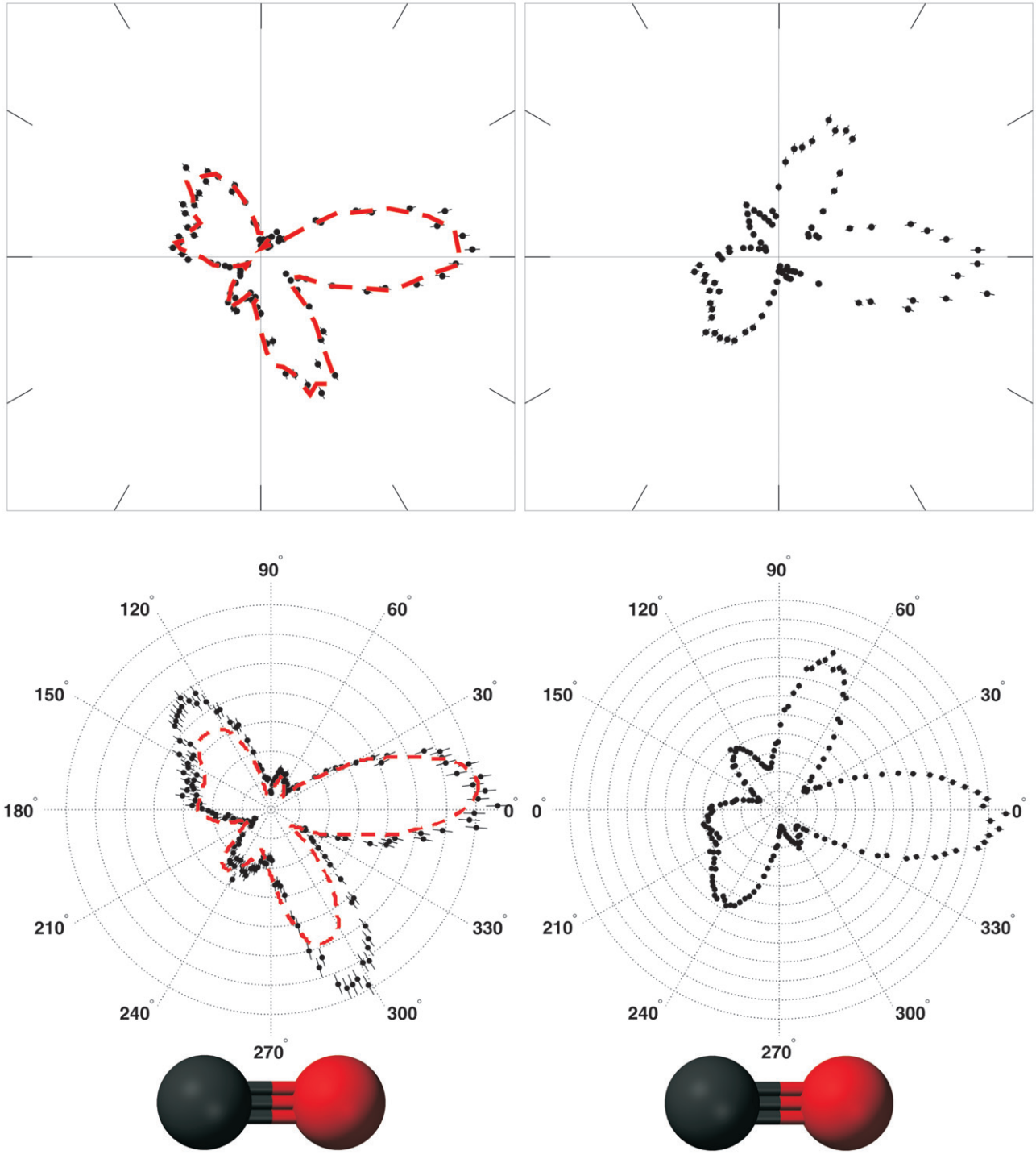

Figure 2. Photoelectron angular distributions in the y–z plane for molecular orientation in the z direction (0–180°) perpendicular to the incoming photon momentum and angular momentum vector. The molecular fragmentation axis is horizontal with the carbon on the left. Only fragment channels with KER > 11 eV are selected, which ensures the validity of the axial recoil approximation [20]. Left: left circular polarized; and right: right circular polarized photons (upper part, Jahnke *et al.* [20,21]; lower part, this work). The red dashed line in the left figures represents the 'guided by the eyes' distributions in the right figures mirrored in the z-axis.

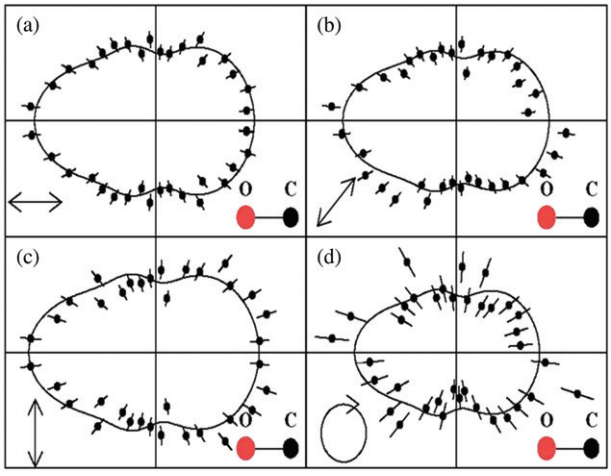

Figure 3. Angular distribution of Auger electrons from the narrow $^1\Sigma^+$ line at 250.5 eV [13,22]. The orientation of the molecule is horizontal with the oxygen to the left as indicated. (a)–(c) Linear polarized light; the polarization vector is indicated by the double-headed arrow, propagating into the plane of the figure. (d) Circular polarized light, propagating into the plane of the figure. Note that, for this state, the KER lies in the energy window B of Figure 4 and the molecule is known to rotate before fragmentation [22].

corresponds to such fast fragmentation processes, whereas for smaller KER the fragmentation is delayed (see also Ref. [24]). Our present data for a KER of C^+ and O^+ ranging from 11 to 16 eV are in good agreement with the findings of Jahnke *et al.* (see Figure 2). The photoelectrons are primarily emitted in the plane perpendicular to the photon momentum. Our present angular distribution is, however, rotated slightly by approximately 5–7° compared with the measurement of Jahnke. This small rotation is probably due to a slight misalignment between the axes of the magnetic field and the electric field inside the spectrometer.

Weber *et al.* [13,22] measured, for the same fragmentation process, the carbon K-shell Auger electron emission with respect to the molecular orientation for linear as well as left and right circularly polarized light, but without coincident detection of the photoelectron (Figure 3). They found a strongly aligned emission in the direction of the molecular axis. Jahnke and Weber did not detect all four fragments in coincidence and could therefore not explore the vector correlation of the four-particle emission.

Our present data for lower KER values, i.e. other long-living fragmentation channels with molecular rotation, are shown in Figure 4. Due to a delayed Coulomb explosion, the molecular axis has rotated slightly and thus the well-pronounced interference structure of Figure 2 is somewhat smeared out, but the maxima in the distribution still remain at the same angular position.

The lower part of Figure 4 shows the Auger electron distributions from our present experiment summed over the ion emission in both z directions (i.e. aligned but not orientated molecules). For the lower KER intervals B and C we find good agreement with the data of Weber *et al.*, but for KER interval A the distribution shows a clear asymmetry with respect to the molecular axis. We currently have no explanation for this asymmetry. One might suspect a possible slight misalignment of the electric and magnetic fields which rotates the Auger electron distribution. Moreover, the supersonic gas jet has a momentum off-set in the $+y$ direction of a few a.u., which may affect the symmetry in the y–z plane. If this were the case, however, the Auger electron distributions shown for KER windows B and C should show the same influence and asymmetry, but they do not.

When this measurement was performed it was not the goal to investigate these vector correlations. Thus perfect control of the fragment trajectories in the superimposed magnetic and electric field configuration was not the primary focus. Therefore, we cannot exclude small unknown experimental uncertainties in the determination of the particle trajectories. Because of these uncertainties we will not present the complete set of our highly differential vector correlation data to avoid speculation on symmetry breaking. In Figure 5 we only present one subset of the data, which indicates the puzzle concerning the measured electron distributions with respect to the measured vector correlation. Between the left and right parts of Figure 5 the circular polarization is changed ($t \rightarrow -t$) and the ion vector is inverted ($\mathbf{n} \rightarrow -\mathbf{n}$), but no indication of any symmetry is found for the Auger electron distribution. The photoelectron distributions, however, show nearly perfect symmetry with respect to left and right circular polarized photons. This can be seen from the red dashed lines shown in the figures for left circular polarized photons in Figures 2 and 5, which represent the distribution lines ('to guide the eyes') for right circular polarized photons. The strong asymmetry for the Auger emission is indeed an unexpected and surprising result. But because of the possible small experimental uncertainties in the direction of the electric and magnetic fields, no conclusion on this finding will be presented here. Rather, we must re-measure these fragmentation processes with improved experimental control of the detection efficiencies and the orientations of the magnetic and electric fields. For comparison, the photoelectron distribution

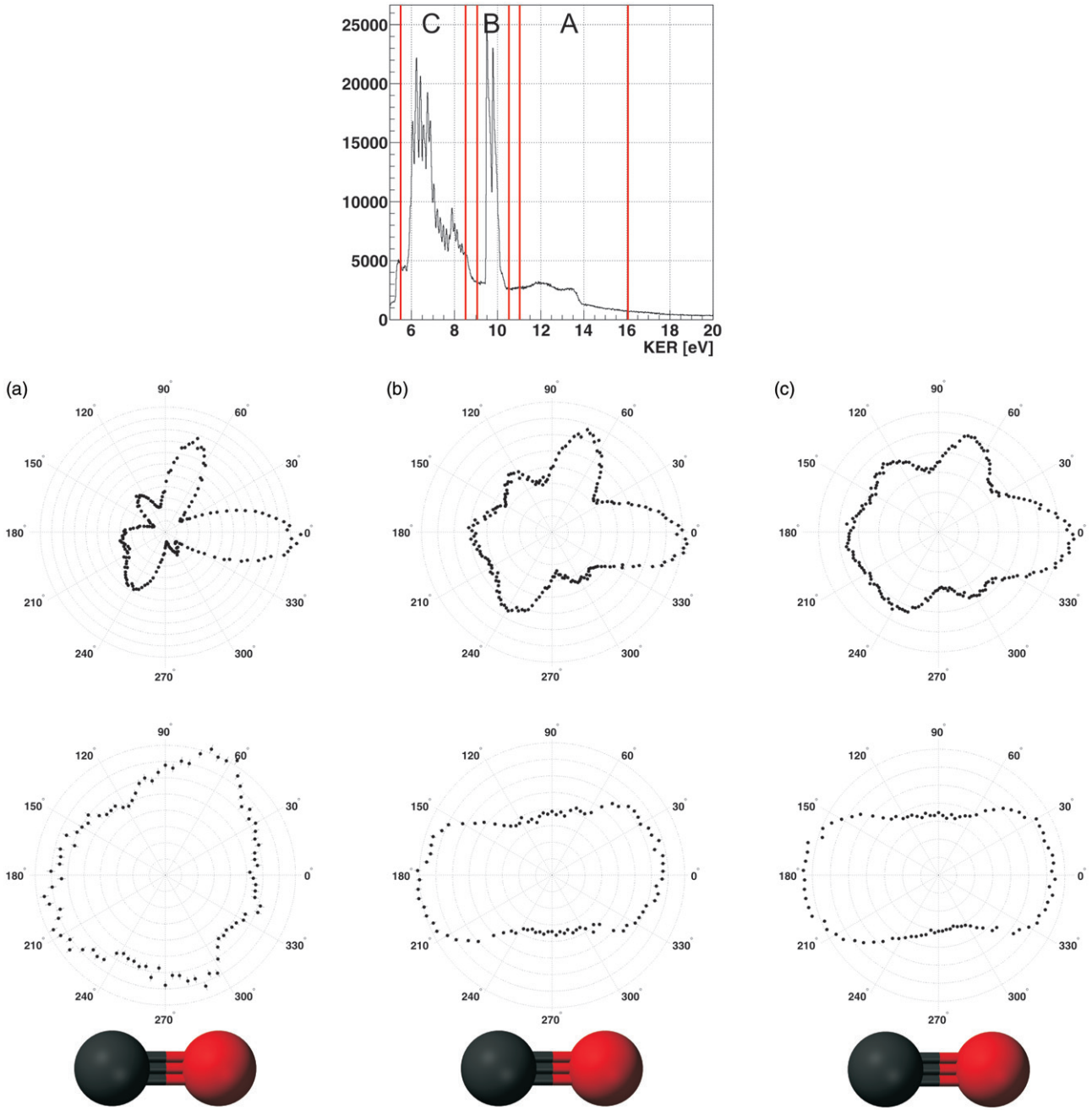

Figure 4. Electron distributions for right circular polarized photons in the y–z plane. Middle: photoelectrons. Bottom: Auger electrons. Top: measured KER value distribution with windows set for photoelectron (upper row) and Auger electron (lower row) distributions. The fragmentation axis (z direction) is horizontal with the carbon on the left. Window A corresponds to fragmentation processes that occur fast enough after photo absorption that rotation of the molecule can be neglected. Windows B and C correspond to fragmentation channels where CO^{2+} lives long enough to partially rotate [22]. The ions were detected in the z direction and the photon momentum and angular momentum point in the x direction.

projected onto the x–z plane is also shown, but no asymmetry is observed. Thus spectrometer misalignment is unlikely in this case.

To motivate the reader to become interested in multiple-fragment vector correlation measurements we conclude with some arguments on possible symmetry tests. What could break the symmetry in the y–z or y'–z' plane? To investigate the symmetry properties in these planes, we can consider the vector $\boldsymbol{Z}$ with $\boldsymbol{Z} = \boldsymbol{A}_{rc\mathrm{photon}} \times \boldsymbol{p}_{\mathrm{ephoto}}$. $\boldsymbol{Z}$ has interesting mirror

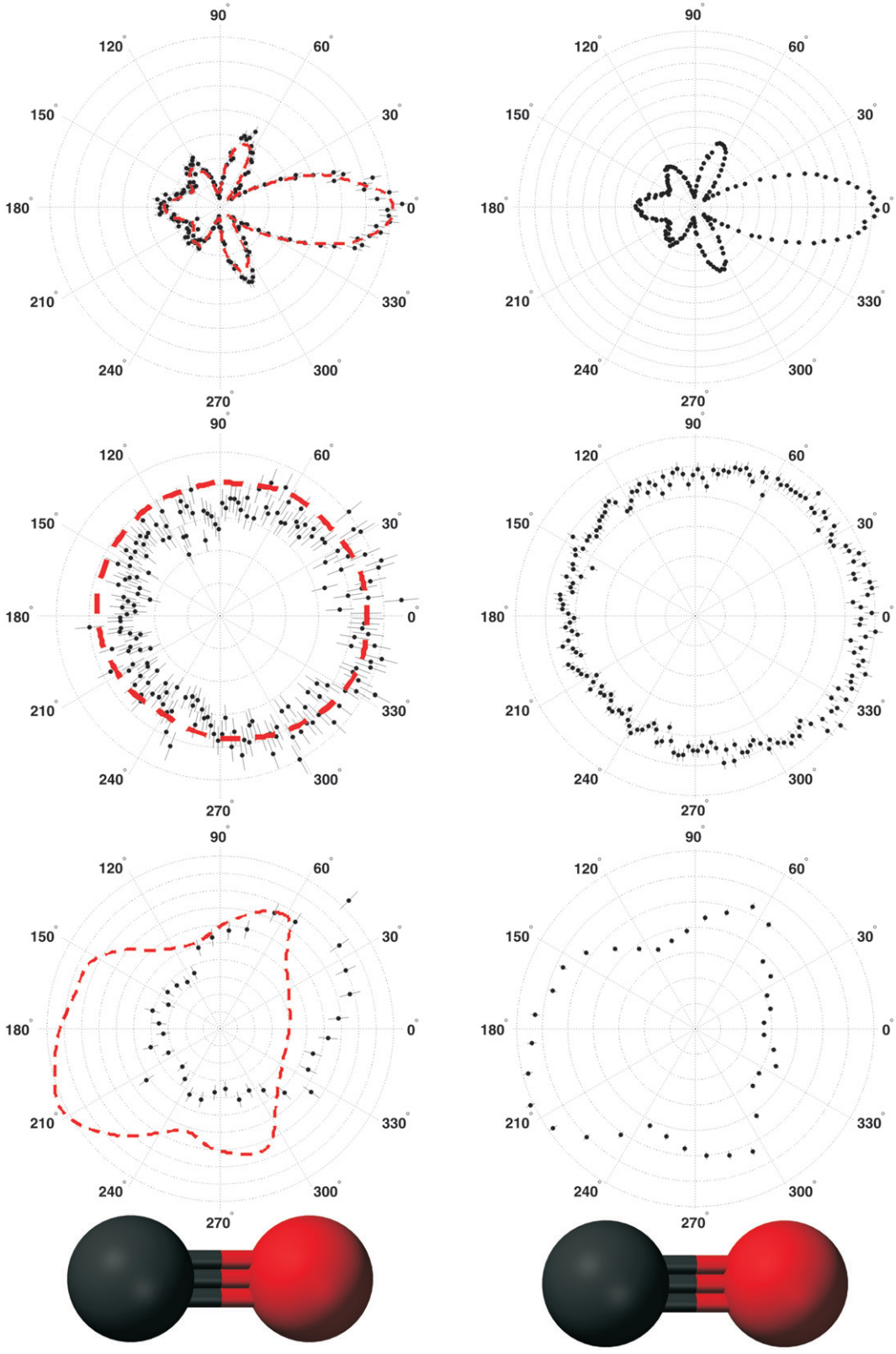

Figure 5. Top: photoelectron distribution projected onto the x–z plane (the vertical is the x direction) for left circular (left side) and right circular polarized photons. Middle: photoelectron distribution projected onto the x–y plane. Bottom: Preliminary Auger electron distributions projected onto the y–z plane. Left: left circular polarized photons and C^+ emission in the $-z$ direction. Right: right polarized photons and C^+ emission in the $+z$ direction. The red dashed lines in the left figures represent the shape of the distributions in the right figures.

properties: after inverting the time $t \rightarrow -t$ the vector $\boldsymbol{Z}(-t)$ still points in the same direction. If instead we invert $\boldsymbol{r} \rightarrow -\boldsymbol{r}$ (parity test), $\boldsymbol{Z}(-\boldsymbol{r})$ points in the *opposite* direction. If the observed asymmetry was a consequence of the symmetry properties of the vector product $\boldsymbol{Z}$, the asymmetry must be associated with the direction of the photoelectron momentum vector and thus change while inverting $\boldsymbol{p}_{\mathrm{ephoto}}$. The first numerical estimates of the effects of space parity non-conservation in the photo and Auger electron spectrum for a number of atoms and ions were made in Ref. [25]. The observation of a left–right asymmetry has been reported for noble gas atoms and H_2 molecules in the interaction with linearly polarized light [26]. Nevertheless, the authors of Ref. [26] recognize that this asymmetry cannot originate from the (fundamental) weak interaction and further experimental work is necessary to investigate the left–right asymmetry in more detail. This may also imply the need for a theoretical model that can describe the observed behavior observed in the present study.

If the asymmetry for carbon monoxide observed here is indeed associated with the properties of the vector $\boldsymbol{Z}$, then replacing $\boldsymbol{A}_{r\mathrm{cphoton}}$ by left polarized light $\boldsymbol{A}_{l\mathrm{cphoton}}$ should change the asymmetry, as the vector $\boldsymbol{Z} = \boldsymbol{A}_{l\mathrm{cphoton}} \times \boldsymbol{p}_{\mathrm{ephoto}}$ now points in the opposite direction. But if it is associated with time inversion, we then also have to invert t by $-t$ in the vector of the Auger emission, which leads to the corresponding transformation of the Auger electron distribution.

4. Outlook and conclusion

Vector correlations measured in four or more particle fragmentation processes are an interesting and powerful tool to investigate possible hidden dynamic symmetries in many-particle systems. State-of-the-art multi-fragment momentum imaging techniques (such as the COLTRIMS reaction microscope) with their excellent momentum resolution and high multi-coincidence efficiency make such measurements feasible. However, to draw reliable conclusions on the symmetry of the measured fragment distributions with respect to vector correlations, one needs careful control of the spectrometer imaging fields, which requires precise field calibration techniques. Also, the detection efficiency for all fragments in all directions must be well calibrated, which is a challenge to experimentalists. The importance of many-particle dynamics in quantum systems makes such investigations crucial to our deeper understanding of the symmetry effects discussed here. Because of the fundamental importance of many-particle dynamics in quantum systems, this challenge must be taken on.

Acknowledgements

We acknowledge the long-term help and support of C.L. Cocke, M.H. Prior and many other colleagues, as well as the support of BMBF, DFG and Roentdek GmbH. M.S. acknowledges financial support from the Alexander von Humboldt foundation. T.A.I. and R.B. acknowledge the Volkswagen Foundation for financial support. We thank the staff of the Advanced Light Source for outstanding support, in particular, by H. Bluhm and T. Tyliszczak from beamline 11.0.2.1. This work is supported by the U.S. Department of Energy (DOE) Basic Energy Sciences under Contract Nos. DE-AC02-05CH11231 and DE-FG02-10ER16146.

References

[1] M. Smolarski, T. Jahnke, S. Schößler, O. Hohn, L.Ph.H. Schmidt, R. Dörner and H. Schmidt-Böcking, *Annual Report of the Institute for Nuclear Physics* (Goethe University, Frankfurt, 2000), p. 25, <http://www.atom.uni-frankfurt.de/publications>.

[2] H. Schmidt-Böcking, Phys. J. **9**, 39 (2010).

[3] D.A. Case and D.R. Herschbach, Mol. Phys. **30**, 1537 (1975); D.A. Case, G.M. McClelland and D.R. Herschbach, Mol. Phys. **35**, 541 (1978); J.D. Barnwell, J.G. Loeser and D.R. Herschbach, J. Phys. Chem. **87**, 2781 (1983); G.M. McClelland and D.R. Herschbach, J. Phys. Chem. **91**, 5509 (1987).

[4] M. Lemeshko, P.G. Jambrina, M.P. de Miranda and B. Friedrich, J. Chem. Phys. **132**, 161102 (2010).

[5] F. Trinter, Master's thesis, Goethe University Frankfurt, 2011. <http://www.atom.uni-frankfurt.de/publications>.

[6] J. Ullrich, R. Moshammer, A. Dorn, R. Dörner, L.Ph.H. Schmidt and H. Schmidt-Böcking, Rep. Prog. Phys. **66**, 1463 (2003).

[7] T. Jahnke, Th. Weber, T. Osipov, A.L. Landers, O. Jagutzki, L.Ph.H. Schmidt, C.L. Cocke, M.H. Prior, H. Schmidt-Böcking and R. Dörner, J. Electron Spectrosc. Relat. Phenom. **141**, 229 (2004).

[8] R. Dörner, V. Mergel, O. Jagutzki, L. Spielberger, J. Ullrich, R. Moshammer and H. Schmidt-Böcking, Phys. Rep. **330**, 95 (2000).

[9] L.Ph.H. Schmidt, S. Schößler, F. Afaneh, M.S. Schöffler, K. Stiebing, H. Schmidt-Böcking and R. Dörner, Phys. Rev. Lett. **101**, 173202, and private communication (2008).

[10] M.S. Schöffler, J. Titze, N. Petridis, T. Jahnke, K. Cole, L.Ph.H. Schmidt, A. Czasch, D. Akoury, O. Jagutzki, J.B. Williams, N.A. Cherepkov, S.K. Semenov, C.W. McCurdy, T.N. Rescigno, C.L. Cocke, T. Osipov, S. Lee, M.H. Prior, A. Belkacem, A.L. Landers, H. Schmidt-Böcking, Th. Weber and R. Dörner, Science **320**, 920 (2008).

[11] V.V. Kuznetsov and N.A. Cherepkov, J. Electron Spectrosc. Relat. Phenom. **79**, 437 (1996).

[12] R. Guillemin, E. Shigemasa, K.L. Guen, D. Ceolin, C. Miron, N. Leclerq, P. Morin and M. Simon, Phys. Rev. Lett. **87**, 203001 (2001).

[13] Th. Weber, M. Weckenbrock, M. Balser, L.Ph.H. Schmidt, O. Jagutzki, W. Arnold, O. Hohn, M.S. Schöffler, E. Arenholz, T. Young, T. Osipov, L. Foucar, A. De Fanis, R. Diez Muino, H. Schmidt-Böcking, C.L. Cocke, M.H. Prior and R. Dörner, Phys. Rev. Lett. **90**, 153003 (2003).
[14] F. Roubichaux, private communication.
[15] A. Czasch, L.Ph.H. Schmidt, T. Jahnke, Th. Weber, O. Jagutzki, S. Schößler, M.S. Schöffler, R. Dörner and H. Schmidt-Böcking, Phys. Lett. A **347**, 95 (2005).
[16] M.S. Schöffler, T. Jahnke, J. Titze, N. Petridis, K. Cole, L. Ph., H. Schmidt, A. Czasch, O. Jagutzki, J.B. Williams, C.L. Cocke, T. Osipov, S. Lee, M.H. Prior, A. Belkacem, A.L. Landers, H. Schmidt-Böcking, R. Dörner and Th. Weber, New J. Phys. **13**, 095013 (2011).
[17] R. Moshammer, M. Unverzagt, W. Schmitt, J. Ullrich and H. Schmidt-Böcking, Nucl. Instrum. Meth. B **108**, 425 (1996).
[18] E.S. Shuman, J.F. Barry and D. DeMille, Nature **467**, 820 (2010).
[19] T.A. Isaev, S. Hoekstra and R. Berger, Phys. Rev. A **82**, 052521 (2010).
[20] T. Jahnke, Th. Weber, A.L. Landers, A. Knapp, S. Schößler, J. Nickles, S. Kammer, O. Jagutzki, L.Ph.H. Schmidt, A. Czasch, T. Osipov, E. Arenholz, A.T. Young, R. Diez Muino, D. Rolles, F.J. Garcia de Abajo, C.S. Fadley, M.A. Van Hove, S.K. Semenov, N.A. Cherepkov, J. Rösch, M.H. Prior, H. Schmidt-Böcking, C.L. Cocke and R. Dörner, Phys. Rev. Lett. **88**, 073002 (2002).
[21] T. Jahnke, J. Titze, L. Foucar, R. Wallauer, T. Osipov, E.P. Benis, O. Jagutzki, W. Arnold, A. Czasch, A. Staudte, M.S. Schöffler, A. Alnaser, Th. Weber, M.H. Prior, H. Schmidt-Böcking and R. Dörner, J. Electron Spectrosc. Relat. Phenom. **183**, 48 (2011).
[22] Th. Weber, O. Jagutzki, M. Hattass, A. Staudte, A. Nauert, L.Ph.H. Schmidt, M.H. Prior, A.L. Landers, A. Bräuning-Demian, H. Bräuning, C.L. Cocke, T. Osipov, I. Ali, R. Diez Muino, D. Rolles, F.J. Garcia de Abajo, C.S. Fadley, M.A. Van Hove, A. Cassimi, H. Schmidt-Böcking and R. Dörner, J. Phys. B **34**, 3669 (2001).
[23] R.N. Zare, Mol. Photochem. **4**, 1 (1972).
[24] T. Osipov, C.L. Cocke, M.H. Prior, A.L. Landers, Th. Weber, O. Jagutzki, L.Ph.H. Schmidt, H. Schmidt-Böcking and R. Dörner, Phys. Rev. Lett. **90**, 233002 (2003).
[25] L.N. Labzovsky and M. Melibaev, J. Phys. B: Atom. Molec. Phys. **12**, 2115 (1979).
[26] S. Ricz, T. Ricsoka, A. Köver, D. Varga, M. Huttula, S. Urpelainen, H. Aksela and S. Aksela, New J. Phys. **9**, 274 (2007).